

# Phenomenology of Trinification models

João Seabra (n.76141)<sup>1</sup>

<sup>1</sup>*Departamento de Física, Instituto Superior Técnico, Universidade de Lisboa, Lisboa, Portugal*

Trinification models, like other proposed Grand Unified Theories, may be able to provide us a better understanding of elementary particles and their interactions. Namely, the appearance of vectorlike quarks in this class of models may lead to new sources of CP violation. After a brief recap of the Standard Model, we review some of the main properties of vectorlike quarks and current experimental constraints. Then, we study the phenomenology of Trinification models and the possibility of implementing spontaneous CP violation. We show that the mixing among vectorlike and Standard Model quarks leads to a complex CKM matrix in agreement with experimental data.

## I. Introduction

Most of our current understanding about elementary particles and how they interact through electromagnetic, weak and strong interactions is embodied in the Standard Model (SM) of particle physics. With the discovery of the Higgs Boson in 2012 at the Large Hadron Collider (LHC), all of the particles in the SM have been observed and experimental data supports most of its predictions. However, the SM cannot be regarded as a complete theory and, therefore, it must be extended in order to explain some observed phenomena. For example, the SM is not able to account for neutrino oscillations (an experimental proof that neutrinos are massive particles), it does not contain any dark matter candidate and it is unable to explain the matter-antimatter asymmetry of the universe. This last fact is deeply connected with the breaking of the symmetry Charge conjugation and Parity (CP) [1].

Possible extensions to the SM that can provide an answer for some of the above open questions are provided by Grand Unified Theories (GUTs), in which the electromagnetic, weak and strong interactions are unified into a single force at some high energy. As a consequence, GUTs rely on a larger gauge group that embeds the SM one, implying the existence of new particles.

In this work, we will study a GUT proposed for the first time by Georgi, Glashow and Rújula, known as Trinification model [2]. This model is based on the trinification group  $SU(3)_c \otimes SU(3)_L \otimes SU(3)_R$ , which is a maximal subgroup of  $E_6$ , with an imposed discrete symmetry  $Z_3$  that ensures the existence of only one gauge coupling constant at high energy. In particular, we will study how the existence of vectorlike quarks in these models may lead to new sources of CP violation.

Vectorlike quarks are hypothetical spin 1/2 particles which transform as triplets under the color gauge group. In contrast with SM quarks, their left and right-handed components transform equally under the  $SU(2)_L$  group. Not only in Trinification models but also in other GUTs based on the group  $E_6$ , vectorlike quarks naturally arise from assigning each generation of fermions to the fundamental representation of  $E_6$ . One of the most important properties of these particles is that they can mix with SM quarks, leading to new sources of CP violation. This

mixing must obey to experimental constraints [3] which we will summarize later.

This work is organized as follows: in Section II we present a brief review of the SM, focusing on the quark sector of the theory, from which CP violation arises. In this context, we present experimental data related to the Cabibbo-Kobayashi-Maskawa (CKM) matrix. In Section III, we review some experimental constraints on the vectorlike quarks masses and their mixing with the third generation SM quarks. In Section IV we present some of the most important features of Trinification models and we show that spontaneous CP violation (SCPV) may be realized. After that, we study in Section V the fermion sector of the theory, giving special attention to quark masses and mixing. Finally, in Section VI we draw the main conclusions of our work.

## II. Brief review of the Standard Model

Before spontaneous symmetry breaking (SSB), the SM is characterized by the gauge group

$$SU(3)_c \otimes SU(2)_L \otimes U(1)_Y. \quad (1)$$

In this work, we consider  $Q = T_3 + Y$  for the electric charge  $Q$ , where  $Y$  is the weak hypercharge and  $T_3$  the third component of weak isospin. We conclude by counting the number of generators of the gauge group that there are twelve gauge fields in the SM to ensure invariance under the gauge group. All of them are massless before SSB, which is realized as:

$$SU(3)_c \otimes SU(2)_L \otimes U(1)_Y \rightarrow SU(3)_c \otimes U(1)_{\text{em}}. \quad (2)$$

Upon SSB driven by the Higgs field  $\Phi$ , three of the gauge fields ( $W_\mu^\pm$  and  $Z_\mu$ ) become massive. On the other hand, the existence of an unbroken  $U(1)_{\text{em}}$  symmetry after SSB (which is identified with the gauge group of electromagnetism) is associated to the existence of a massless gauge field  $A_\mu$  (the photon). Finally, the color group  $SU(3)_c$  remains unbroken, hence the remaining eight gauge fields (gluons) are massless.

In the scalar sector of the SM, the  $SU(2)_L$  invariant Higgs potential is

$$V(\Phi) = \mu^2 \Phi^\dagger \Phi + \lambda (\Phi^\dagger \Phi)^2, \quad (3)$$

where  $\Phi$  is the scalar Higgs doublet, which has hypercharge 1/2 and is defined by

$$\Phi = \begin{pmatrix} \phi^+ \\ \phi^0 \end{pmatrix} \equiv \frac{1}{\sqrt{2}} \begin{pmatrix} \xi_1 + i\xi_2 \\ \xi_3 + i\xi_4 \end{pmatrix}. \quad (4)$$

In order to find the minimum of the potential presented in Eq. (3), we need to solve the equation

$$\frac{\partial V(\Phi)}{\partial \Phi} = 0, \quad (5)$$

which only has a non-zero solution when  $\lambda > 0$  and  $\mu^2 < 0$ . It is straightforward to see that the potential  $V(\Phi)$  is minimized at

$$\langle \Phi \rangle = \begin{pmatrix} 0 \\ v \end{pmatrix}, \quad v = \sqrt{-\frac{\mu^2}{2\lambda}}, \quad (6)$$

breaking the  $SU(2)_L \otimes U(1)_Y$  symmetry into  $U(1)_{\text{em}}$ . We say in this case that the Higgs field acquires a vacuum expectation value (VEV)  $v$ . Considering small oscillations around the vacuum,  $\Phi$  can be reparametrized as

$$\Phi(x) = e^{i\tau_a \xi^a(x)} \begin{pmatrix} 0 \\ v + \frac{H(x)}{\sqrt{2}} \end{pmatrix}, \quad (7)$$

where  $\tau_a$  ( $a = 1, 2, 3$ ) are the Pauli matrices. Performing an  $SU(2)$  transformation to take us to the unitary gauge, the Higgs field can be written as

$$\Phi'(x) = e^{-i\tau_a \xi^a(x)} \Phi(x) = \begin{pmatrix} 0 \\ v + \frac{H(x)}{\sqrt{2}} \end{pmatrix}, \quad (8)$$

where  $H(x)$  is the physical Higgs boson field, the only scalar field that acquires mass. The remaining three scalar fields are 'would-be' Goldstone bosons, which in the present gauge become longitudinal polarizations of the fields  $W_\mu^\pm$  and  $Z_\mu$ .

Finally, in the fermion sector, both leptons and quarks are distributed in three families with identical properties, differing only in their masses. Starting by the leptonic sector, we distribute particles in each family through the following representations of  $SU(2)_L$ :

$$\ell_{iL} = \begin{pmatrix} \nu_{l_i} \\ l_i \end{pmatrix}_L, \quad l_{iR}, \quad (9)$$

where  $l_i = e, \mu, \tau$  is the charged lepton of the family  $i$  and  $\nu_{l_i}$  the corresponding neutrino. As in Eq. (9), we will use  $L$  and  $R$  to distinguish left from right-handed fields, respectively. Each left-handed doublet  $\ell_{iL}$  has  $Y = -1/2$  while right-handed lepton singlets have  $Q = Y = -1$ . In the SM there are no right-handed neutrinos, meaning that there is no lepton mixing and, consequently, there is no CP violation in the leptonic sector of the SM. In the quark sector, particles from each family are distributed in a similar way in terms of  $SU(2)_L$  representations:

$$q_{iL} = \begin{pmatrix} u_i \\ d_i \end{pmatrix}_L, \quad u_{iR}, \quad d_{iR}. \quad (10)$$

Here,  $u_i = u, c, t$  designates the up-quark of family  $i$  with charge  $Q = 2/3$  and  $d_i = d, s, b$  the down-quark, with charge  $Q = -1/3$ . We have again left-handed particles grouped in  $SU(2)_L$  doublets  $q_{iL}$ , but in this case, all quarks have a right-handed component, allowing the occurrence of CP violation in this sector.

We now focus on the terms of the SM Lagrangian associated to quarks. These particles can interact with gauge bosons, originating charged currents (CC) and neutral currents (NC). They are described by the Lagrangians  $\mathcal{L}_{\text{CC}}^q$  and  $\mathcal{L}_{\text{NC}}^q$ ,

$$\mathcal{L}_{\text{CC}}^q = -\frac{g}{\sqrt{2}} \bar{u}_{iL} \gamma^\mu d_{iL} W_\mu^+ + \text{H.c.}, \quad (11)$$

$$\mathcal{L}_{\text{NC}}^q = e \sum_{\psi_i = u_i, d_i} Q(\psi_i) \bar{\psi}_i \gamma^\mu \psi_i A_\mu + \frac{g}{\cos \theta_W} \sum_{\psi_i = u_i, d_i} \bar{\psi}_i \gamma^\mu (g_V^i - g_A^i \gamma_5) \psi_i Z_\mu, \quad (12)$$

respectively. In Eq. (11), H.c. stands for 'Hermitian conjugate' and in Eq. (12), the vector ( $V$ ) and axial ( $A$ ) couplings for the fermion  $i$  are given by

$$g_V^i \equiv T_3^i - 2Q_i \sin^2 \theta_W, \quad g_A^i \equiv T_3^i. \quad (13)$$

In the SM, all quarks and charged leptons acquire mass after SSB due to their Yukawa interactions with the scalar doublet,  $\Phi$ . For quarks, these interactions are encoded in the Yukawa Lagrangian,

$$-\mathcal{L}_{\text{Yuk}}^q = Y_{ij}^u \bar{q}_{iL} \bar{\Phi} u_{jR} + Y_{ij}^d \bar{q}_{iL} \Phi d_{jR} + \text{H.c.}, \quad (14)$$

where  $\bar{\Phi} = i\tau_2 \Phi^*$ , and  $Y_{ij}^u$  and  $Y_{ij}^d$  are general Yukawa coupling matrices. Replacing  $\Phi$  by  $\langle \Phi \rangle$  as in Eq. (6), one gets the mass Lagrangian  $\mathcal{L}_{\text{mass}}^q$ ,

$$-\mathcal{L}_{\text{Mass}}^q = \bar{u}_{iL} M_{ij}^u u_{jR} + \bar{d}_{iL} M_{ij}^d d_{jR} + \text{H.c.}, \quad (15)$$

with  $M_{ij}^u = v Y_{ij}^u$  and  $M_{ij}^d = v Y_{ij}^d$ . By performing bi-unitary transformation of the quark fields,

$$\begin{aligned} u_L &\rightarrow V_L^u u'_L, & d_L &\rightarrow V_L^d d'_L, \\ u_R &\rightarrow U_R^u u'_R, & d_R &\rightarrow U_R^d d'_R, \end{aligned} \quad (16)$$

such that

$$\begin{aligned} V_L^{u\dagger} M^u U_R^u &= \text{diag}(m_u, m_c, m_t), \\ V_L^{d\dagger} M^d U_R^d &= \text{diag}(m_d, m_s, m_b), \end{aligned} \quad (17)$$

the Lagrangian of Eq. (15) becomes

$$-\mathcal{L}_{\text{Mass}} = \sum_{\psi = u_i, d_i} (m_{u_i} \bar{u}'_{iL} u'_{iR} + m_{d_i} \bar{d}'_{iL} d'_{iR}) + \text{H.c.} \quad (18)$$

Implementing the field rotation (16) in the Lagrangian of Eq. (12), we conclude that the NC Lagrangian is invariant under those transformations, meaning that there are no flavor changing neutral currents (FCNCs) at tree

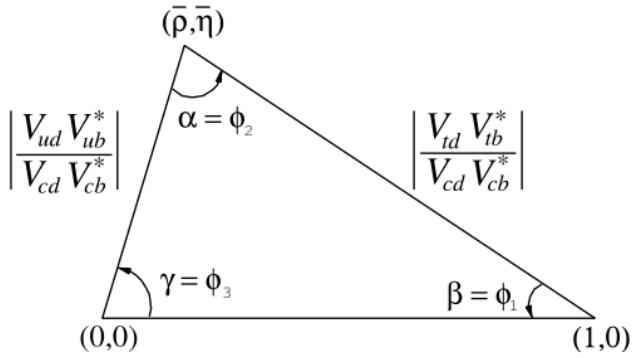


FIG. 1: Sketch of the unitarity triangle (taken from [8]).

level in the SM. As for the CC Lagrangian of Eq. (11), we get

$$\mathcal{L}_{CC}^q = \frac{g}{\sqrt{2}} \bar{u}'_{iL} \gamma^\mu (V_{CKM})_{ij} d'_{jL} W_\mu^+ + \text{H.c.}, \quad (19)$$

where  $V_{CKM}$  is the CKM matrix [4, 5], defined by

$$V_{CKM} \equiv V_L^{u\dagger} V_L^d = \begin{pmatrix} V_{ud} & V_{us} & V_{ub} \\ V_{cd} & V_{cs} & V_{cb} \\ V_{td} & V_{ts} & V_{tb} \end{pmatrix}. \quad (20)$$

In order to parametrize this matrix with three generations of quarks, we need three angles and one phase, which violates CP. Here, we consider the Wolfenstein parametrization [6] for the CKM matrix,

$$V_{CKM} = \begin{pmatrix} 1 - \frac{1}{2}\lambda^2 & \lambda & A\lambda^3(\rho - i\eta) \\ -\lambda & 1 - \frac{1}{2}\lambda^2 & A\lambda^2 \\ A\lambda^3(1 - \rho - i\eta) & -A\lambda^2 & 1 \end{pmatrix} + \mathcal{O}(\lambda^4). \quad (21)$$

As noted in [7], one can also write Eq. (21) in terms of the variables  $\bar{\rho}$  and  $\bar{\eta}$ , defined by  $\bar{\rho} + i\bar{\eta} = -(V_{ud}V_{ub}^*)/(V_{cd}V_{cb}^*)$ . The CKM matrix written in terms of  $\lambda$ ,  $A$ ,  $\bar{\rho}$  and  $\bar{\eta}$  is unitary to all orders in the parameter  $\lambda$ .

As a consequence of the unitarity of  $V_{CKM}$ , the relations  $\sum_i V_{ij}V_{ik}^* = \delta_{jk}$  and  $\sum_i V_{ij}V_{ik}^* = \delta_{jk}$  hold. The orthogonality conditions can be represented as triangles in the  $(\bar{\rho}, \bar{\eta})$  plane. These are known as unitarity triangles, being their areas equal to  $J/2$ , where  $J$  is the Jarlskog invariant  $J$  defined by

$$\text{Im} [V_{ij}V_{kl}V_{il}^*V_{kj}^*] = J \sum_{m,n} \epsilon_{ikm}\epsilon_{jln}. \quad (22)$$

The most commonly used unitarity triangle (represented in Fig. 1) arises from

$$V_{ud}V_{ub}^* + V_{cd}V_{cb}^* + V_{td}V_{tb}^* = 0, \quad (23)$$

where we normalize each term to  $V_{cd}V_{cb}^*$ .

Parameter	Fit
$\lambda$	$0.22506 \pm 0.00050$
$A$	$0.811 \pm 0.026$
$\bar{\rho}$	$0.124^{+0.019}_{-0.018}$
$\bar{\eta}$	$0.356 \pm 0.011$

TABLE I: Fit results for the Wolfenstein parameters. These values were obtained using the method described in [8].

In Table I, we present the fit for the Wolfenstein parameters. The fit results for the magnitude of all nine CKM matrix elements, presented in Eq. (20), are

$$V_{CKM} = \begin{pmatrix} 0.97434^{+0.00011}_{-0.00012} & 0.22506 \pm 0.00050 & 0.00357 \pm 0.00015 \\ 0.22492 \pm 0.00050 & 0.97351 \pm 0.00013 & 0.0411 \pm 0.0013 \\ 0.00875^{+0.00032}_{-0.00033} & 0.0403 \pm 0.0013 & 0.99915 \pm 0.00005 \end{pmatrix}, \quad (24)$$

leading to the Jarlskog invariant,  $J = (3.04^{+0.21}_{-0.20}) \times 10^{-5}$ . Finally, the global fit result is illustrated in Fig. 2, where the experimental constraints on all the CP-violating observables are plotted in the  $(\bar{\rho}, \bar{\eta})$  plane. Each shaded area represents the allowed region for an observable in that plane with 95% Confidence Level (CL) and one can check that all those areas overlap consistently around the global fit region.

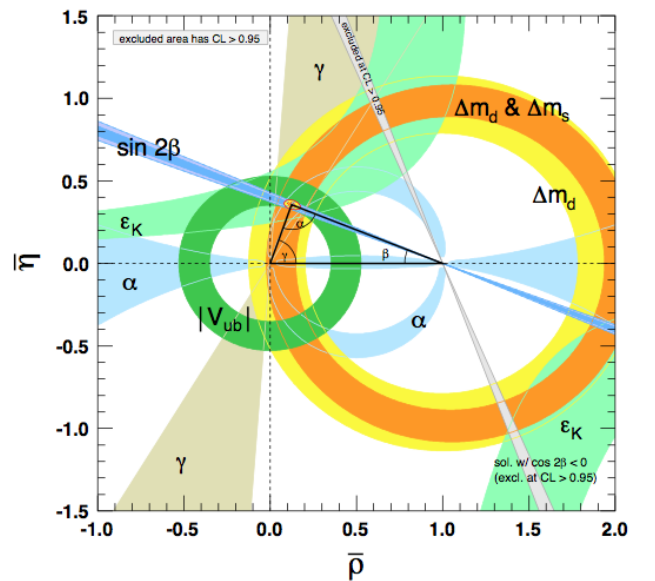


FIG. 2: Experimental constraints on the  $(\bar{\rho}, \bar{\eta})$  plane. The ring centered at  $(0,0)$  establishes the allowed region for the magnitude of the CKM matrix element  $V_{ub}$  and the ones centered at  $(1,0)$  are associated to the mass differences  $\Delta m_d$  and  $\Delta m_s$  between  $B^0$  and  $B_s^0$  mesons, respectively. The hyperbolic curves limit the allowed region of the CP-violating observable in the kaon sector  $\epsilon_K$ . The remaining regions belong to the angles of the unitarity triangle, namely  $\alpha$ ,  $\beta$  and  $\gamma$ . All the shaded areas have 95% CL (image taken from [8]).

### III. Constraints on vectorlike quarks

Recall from Section I that vectorlike quarks are colored fermions whose left and right-handed fields transform identically under  $SU(2)_L$ . While there is no evidence for the existence of these particles, they have been receiving a lot of attention nowadays. Along with the mixing they may develop with SM quarks, they are the simplest example of colored fermions still allowed by experimental data. Indeed, vectorlike quarks do not acquire mass from Yukawa couplings, therefore evading the constraints from Higgs boson production that rule out for example, a fourth generation of SM quarks [9].

In this section, we present the constraints on the mass and mixing of vectorlike quarks. Since trinified models include vectorlike  $B$  quarks with charge  $Q = -1/3$  and singlets of  $SU(2)_L$ , we will focus on this type only<sup>1</sup>. In order to simplify the analysis, we assume that the  $B$  quark of our model couples only to the SM  $b$  one. In fact, we expect dominant  $b - B$  mixing due to the large  $b$  Yukawa coupling in comparison with the  $d$  and  $s$  ones.

The existence of  $b - B$  mixing results in new contributions to the oblique parameters  $S$  and  $T$ , precisely measured at the Large Electron-Positron Collider (LEP) and Stanford Linear Collider (SLC). Designating  $\Delta S = S - S_{\text{SM}}$  and  $\Delta T = T - T_{\text{SM}}$  as the changes in the parameters  $S$  and  $T$  respectively (we consider  $\Delta U = 0$ ), the following experimental values were obtained for these quantities [10],

$$\Delta S = 0.04 \pm 0.07, \quad \Delta T = 0.07 \pm 0.08, \quad (25)$$

with a correlation of 0.88. Other measurements taken into account to constrain the  $b - B$  mixing are those coming from the  $Z \rightarrow b\bar{b}$  decay (also at LEP and SLC). This stems from the fact that this mixing modifies the  $Zb\bar{b}$  coupling at tree level, as well as the SM predictions of four observables. Two of these are  $R_b$  and  $R_c$ , defined as

$$R_b = \frac{\Gamma(Z \rightarrow b\bar{b})}{\Gamma(Z \rightarrow \text{had})}, \quad R_c = \frac{\Gamma(Z \rightarrow c\bar{c})}{\Gamma(Z \rightarrow \text{had})}, \quad (26)$$

where  $\Gamma(Z \rightarrow \text{had})$  is the decay of  $Z$  boson into hadrons (excluding the top quark). The remaining two are the Forward-Backward (FB) asymmetry  $A_{\text{FB}}^b$  and the asymmetry parameter  $A_b$ , both associated to the  $b$  quark,

$$A_{\text{FB}}^b = \frac{3}{4} A_b \frac{A_e + P_e}{1 + P_e A_e}, \quad A_b = \frac{2\bar{g}_V^b \bar{g}_A^b}{\bar{g}_V^{b^2} + \bar{g}_A^{b^2}}, \quad (27)$$

where  $\bar{g}_V^b$  and  $\bar{g}_A^b$  are the effective couplings, which include electroweak radiative corrections. The parameter

<sup>1</sup> Most of the information shown in this section is also presented in [3], where it can be found more details about vectorlike quarks and their experimental constraints.

Parameter	SM	Experimental
$R_b$	0.21576	$0.21629 \pm 0.00066$
$A_b$	0.9348	$0.923 \pm 0.020$
$A_{\text{FB}}^b$	0.1034	$0.0992 \pm 0.0016$
$R_c$	0.17227	$0.1721 \pm 0.003$

TABLE II: SM predictions [10] and experimental results [11] for the observables affected by the  $Zb\bar{b}$  coupling.

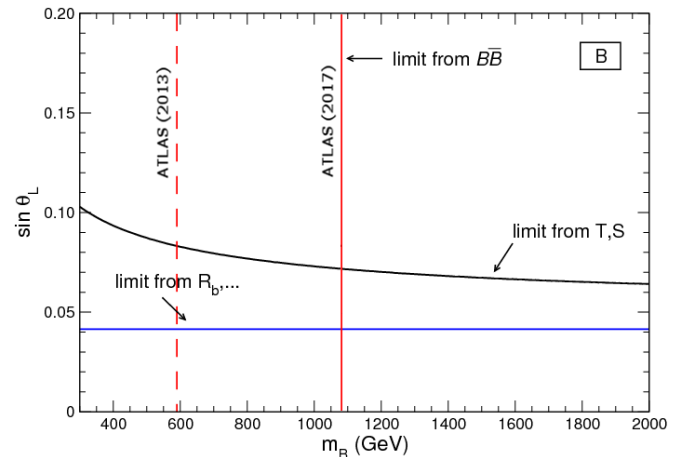


FIG. 3: Constraints to the mixing angle  $\theta_L$  as a function of the vectorlike  $B$  quark mass. The black line represents the constraints due to the change in the oblique parameters  $S$  and  $T$  and the blue line the constraints related to the observables  $R_b$ ,  $R_c$ ,  $A_{\text{FB}}^b$  and  $A_b$ , affected by the change in the  $Zb\bar{b}$  vertex. The vertical dashed and continuous red lines indicate the limit imposed by the ATLAS collaboration in 2013 [14] and 2017 [13] respectively (image adapted from [3]).

$A_e$  is similar to  $A_b$  with the replacement  $b \rightarrow e$ , and  $P_e$  is the initial  $e^-$  polarization.

In Table II, we show the SM predictions for the observables shown in Eqs. (26) and (27), as well as their experimental values. In Fig. 3 we present constraints imposed to  $\theta_L$  (the mixing angle between the left-handed  $b$  and  $B$  quarks). As shown in [12], its relation with the mixing angle in the right-handed sector  $\theta_R$  is given by

$$\tan \theta_R = \frac{m_b}{m_B} \tan \theta_L, \quad (28)$$

where  $m_b$  and  $m_B$  are the masses of  $b$  and  $B$  quarks, respectively. This allows us to conclude that the mixing angle  $\theta_L$  dominates towards  $\theta_R$  for the vectorlike quark that we are studying. We also present the current lower mass limit (continuous red line) for the mass of the  $B$  quark. This has been obtained through searches of pair production of vectorlike quarks [13], resulting in  $m_B > 1080$  GeV. As noted in [3], this constraint depends on the possible decay modes of the  $B$  quark into SM particles:  $B \rightarrow W^- t$ ,  $B \rightarrow Z b$  and  $B \rightarrow H b$ .

#### IV. General Properties of Trinification models

As mentioned in Section I, Trinification models are characterized by the gauge group  $SU(3)_c \otimes SU(3)_L \otimes SU(3)_R$ , where we identify  $SU(3)_c$  as the unbroken color group,  $SU(3)_L$  the one containing the  $SU(2)_L$  group of the SM and  $SU(3)_R$  the right-handed analog of  $SU(3)_L$ . We consider that at the unification scale  $M_u \sim 10^{14}$  GeV [15], the trinification group breaks down spontaneously to the SM group. However, other possibilities can be considered [16], where the trinification group breaks down to  $SU(3)_c \otimes SU(2)_L \otimes SU(2)_R \otimes U(1)_{B-L}$  ( $B-L$  represents the difference between baryon and lepton number) before breaking to the SM gauge group.

The trinification group contains two representations to which particles may be assigned: the adjoint representation, with dimension 24,

$$\mathbf{24} \rightarrow (\mathbf{8}, \mathbf{1}, \mathbf{1}) \oplus (\mathbf{1}, \mathbf{8}, \mathbf{1}) \oplus (\mathbf{1}, \mathbf{1}, \mathbf{8}), \quad (29)$$

and the **27** fundamental representation of  $E_6$ , which transforms under the trinification group as follows:

$$\mathbf{27} \rightarrow (\mathbf{1}, \bar{\mathbf{3}}, \mathbf{3}) \oplus (\mathbf{3}, \mathbf{1}, \bar{\mathbf{3}}) \oplus (\bar{\mathbf{3}}, \mathbf{3}, \mathbf{1}). \quad (30)$$

One can verify that both representations are invariant under permutations of the three  $SU(3)$  factors, meaning that a discrete symmetry  $\mathbb{Z}_3$  can be imposed to the model [17]. In fact, this becomes necessary since it guarantees the existence of only one gauge coupling constant at high energies.

In contrast with fermions and scalar particles, gauge bosons are assigned to the representation shown in Eq. (29). Therefore, Trinification models predict the existence of 24 gauge bosons, meaning that there are 12 new heavy gauge bosons that acquire mass through SSB. It can be shown that all the heavy gauge bosons have integer charges, meaning that proton decay cannot be mediated by gauge interactions, as it happens in other GUTs like  $SU(5)$  [18].

The fermion field content is organized in the **27** representation shown in Eq. (30). Representing the lepton, antiquark and quark multiplets by  $\psi_\ell$ ,  $\psi_{\bar{q}_R}$  and  $\psi_{q_L}$  respectively, each family of fermions will be assigned to one of the components of the **27** representation,

$$\mathbf{27} \rightarrow \psi_\ell(\mathbf{1}, \bar{\mathbf{3}}, \mathbf{3}) \oplus \psi_{\bar{q}_R}(\mathbf{3}, \mathbf{1}, \bar{\mathbf{3}}) \oplus \psi_{q_L}(\bar{\mathbf{3}}, \mathbf{3}, \mathbf{1}). \quad (31)$$

Decomposing the fermion multiplets of Eq. (31) with respect to SM gauge group, we get

$$\psi_\ell \rightarrow \left(\mathbf{1}, \mathbf{2}, \frac{1}{2}\right) \oplus 2 \left(\mathbf{1}, \mathbf{2}, -\frac{1}{2}\right) \oplus (\mathbf{1}, \mathbf{1}, 1) \oplus 2(\mathbf{1}, \mathbf{1}, 0), \quad (32)$$

$$\psi_{\bar{q}_R} \rightarrow \left(\bar{\mathbf{3}}, \mathbf{1}, \frac{2}{3}\right) \oplus 2 \left(\bar{\mathbf{3}}, \mathbf{1}, -\frac{1}{3}\right), \quad (33)$$

$$\psi_{q_L} \rightarrow \left(\mathbf{3}, \mathbf{2}, \frac{1}{6}\right) \oplus \left(\mathbf{3}, \mathbf{1}, -\frac{1}{3}\right). \quad (34)$$

This allows us to write the fermion multiplets in the following way:

$$\psi_\ell = \begin{pmatrix} E^0 & E^- & e^- \\ E^+ & \bar{E}^0 & \nu \\ e^+ & N_1 & N_2 \end{pmatrix}, \quad (35)$$

$$\psi_{\bar{q}_R} = \begin{pmatrix} u^c \\ d^c \\ B^c \end{pmatrix}, \quad (36)$$

$$\psi_{q_L} = (u \ d \ B). \quad (37)$$

We observe that trinified models contain several new fermions. In the leptonic sector, there are two new weak doublets: one with the same quantum numbers as the SM weak doublet, formed by the heavy leptons  $E^-$  and  $\bar{E}^0$  (with charge  $-1$  and  $0$  respectively), and another with opposite hypercharge, that we assume to contain  $E^0$  and  $E^+$  (antiparticles of  $\bar{E}^0$  and  $E^-$  respectively). Two neutral lepton singlets  $N_1$  and  $N_2$  are also introduced. In the quark sector, we find in each generation an  $SU(2)_L$  singlet formed by a vectorlike  $B$  quark, as we anticipated in Section III.

Finally, in the scalar sector, the Higgs field is composed by at least two complex scalar fields, both in the **27** representation. Even though it is possible to construct a model based on the Trinification group with more than two scalar fields, we consider here the model that is usually called Minimal Trinification [19]. This version contains only two scalar fields  $\phi$  and  $\chi$ , that break the trinification group down to the SM. There are two reasons that lead us to reject the possibility of having just one scalar field. First, we could always find a gauge in which the VEVs are diagonal, hence we would not be able to break the left-right symmetry displayed by the trinification group. On the other hand, the CKM matrix would be trivial if there would be only one field to which quarks couple to [18].

From Eq. (30), we notice that of the three bitriplets in which the Higgs field is decomposed, two of them are colored. These components of both scalar fields cannot obtain VEV because the color group  $SU(3)_c$  is not broken by SSB. Although we will not study the properties of these particles in detail, it is worth noting that they must have mass of the order of the unification scale and their presence in the theory is important to explain the generation of neutrino masses, either through radiative [19] or inverse [20] seesaw mechanisms. On the other hand, color singlets (which we will denote by  $\phi_c$  and  $\chi_c$ ) are able to obtain VEV, inducing SSB as a consequence. Under the SM gauge group, these scalar fields have the same decomposition as each lepton family in the fermion sector, hence  $\phi_c$  and  $\chi_c$  can be written as multiplets with a

similar structure to the one presented in Eq. (32) for  $\psi_\ell$ :

$$\phi_c = \begin{pmatrix} \Phi_1 & \Phi_2 & \Phi_3 \\ S_1 & S_2 & S_3 \end{pmatrix}, \quad (38)$$

$$\chi_c = \begin{pmatrix} \Phi_4 & \Phi_5 & \Phi_6 \\ S_4 & S_5 & S_6 \end{pmatrix}. \quad (39)$$

While SSB from  $[\text{SU}(3)]^3$  to  $\text{SU}(3)_c \otimes \text{SU}(2)_L \otimes \text{U}(1)_Y$  is induced by the VEVs of the singlets  $S_2, S_3, S_5$  and  $S_6$  ( $S_1$  and  $S_4$  cannot obtain VEV because they are electrically charged), the electroweak symmetry is broken by the VEVs of electrically neutral components of the doublets  $\Phi_i$ . Given this, the most general vacuum configuration for the scalar fields may be written as<sup>2</sup>

$$\langle \phi \rangle = \begin{pmatrix} \hat{v}_1 & 0 & 0 \\ 0 & \hat{v}_2 & 0 \\ 0 & 0 & \hat{M}_1 \end{pmatrix}, \quad (40)$$

$$\langle \chi \rangle = \begin{pmatrix} \hat{b}_1 & 0 & 0 \\ 0 & \hat{b}_2 & \hat{b}_3 \\ 0 & \hat{M}_2 & \hat{M}_3 \end{pmatrix}, \quad (41)$$

where we consider already a gauge in which the VEV of  $\phi$  is diagonal. Given the symmetry breaking pattern described above, we conclude that  $\hat{M}_1, \hat{M}_2$  and  $\hat{M}_3$  are of the order of unification scale, whereas the remaining VEVs are close to the electroweak scale.

We can now write the scalar potential for this model. Since colored components of the Higgs field do not acquire VEV, all terms proportional to them are set to zero (the complete potential is presented in [18]). Hence, the potential is

$$\begin{aligned} V(\phi, \chi) = & -\mu_1^2 \text{Tr}(\bar{\phi}_c \phi_c) + \alpha_1 [\text{Tr}(\bar{\phi}_c \phi_c)]^2 \\ & + \alpha_2 \text{Tr}(\bar{\phi}_c \phi_c \bar{\phi}_c \phi_c) - \mu_2^2 \text{Tr}(\bar{\chi}_c \chi_c) \\ & + \beta_1 [\text{Tr}(\bar{\chi}_c \chi_c)]^2 + \beta_2 \text{Tr}(\bar{\chi}_c \chi_c \bar{\chi}_c \chi_c) \\ & + \lambda_1 \text{Tr}(\bar{\phi}_c \phi_c) \text{Tr}(\bar{\chi}_c \chi_c) + \\ & + \lambda_2 \text{Tr}(\bar{\phi}_c \chi_c) \text{Tr}(\bar{\chi}_c \phi_c) \\ & + [\lambda_3 \text{Tr}(\bar{\phi}_c \chi_c)^2 + \text{H.c.}] \\ & + \lambda_4 \text{Tr}(\bar{\phi}_c \phi_c \bar{\chi}_c \chi_c) + \lambda_5 \text{Tr}(\bar{\phi}_c \chi_c \bar{\chi}_c \phi_c) \\ & + [\lambda_6 \text{Tr}(\bar{\phi}_c \chi_c \bar{\phi}_c \chi_c) + \text{H.c.}] \\ & + [\gamma_1 (\phi_c)_\alpha^i (\phi_c)_\beta^j (\phi_c)_\gamma^k \epsilon_{ijk} \epsilon^{\alpha\beta\gamma} + \text{H.c.}] \\ & + [\gamma_2 (\phi_c)_\alpha^i (\chi_c)_\beta^j (\chi_c)_\gamma^k \epsilon_{ijk} \epsilon^{\alpha\beta\gamma} + \text{H.c.}], \end{aligned} \quad (42)$$

where  $\mu_i$  and  $\gamma_i$  have dimensions of mass and the remaining coefficients are dimensionless. It is possible to obtain

both SCPV and a realistic mass spectrum by considering the following VEVs:

$$\langle \phi \rangle = \begin{pmatrix} 0 & 0 & 0 \\ 0 & v \cos \xi & 0 \\ 0 & 0 & M_1 e^{i\theta} \end{pmatrix}, \quad (43)$$

$$\langle \chi \rangle = \begin{pmatrix} v \sin \xi & 0 & 0 \\ 0 & 0 & 0 \\ 0 & M_2 & M_3 \end{pmatrix}, \quad (44)$$

where  $v = 174$  GeV. With such VEV structure, we can now obtain several constraints to the scalar potential. First, computing the first derivatives of the scalar potential in order to all scalar fields in the minimum of both fields ( $\phi = \langle \phi \rangle$  and  $\chi = \langle \chi \rangle$ ), we get a set of relations between the free parameters of the potential. In this process, one can find a CP-violating minimum characterized by the condition

$$\theta = \frac{\pi}{2} + k\pi, \quad k \in \mathbb{Z}. \quad (45)$$

In order to have SCPV, one must ensure that the minimum described by Eq. (45) is absolute. Then, we also have to impose that the scalar potential is negative ( $V(\phi, \chi) < 0$ ). Finally, we may compute the scalar mass matrices, where their eigenvalues correspond to the mass of the scalar particles. These must not only be real and positive but we must also take into account the prediction made by the Goldstone theorem concerning the number of scalar particles. Of the 36 scalar fields (20 neutral and 16 charged), there are 15 that should be massless, so that all gauge bosons (8 charged and 7 neutral) may become massive, apart from the photon and the gluons. Since it is not possible to obtain the eigenvalues of the scalar mass matrices analytically, we tried first to compute them as an expansion in  $\frac{v}{M}$ ,

$$m_i^2 = M^2 \left[ x_{i_0} + x_{i_1} \frac{v}{M} + x_{i_2} \frac{v^2}{M^2} + \mathcal{O} \left( \frac{v^3}{M^3} \right) \right], \quad (46)$$

where  $v$  and  $M$  are of the order of electroweak and unification scales, respectively. Counting the number of vanishing eigenvalues at leading-order in  $\frac{v}{M}$  of the mass matrices of neutral and charged scalar particles, we concluded that two neutral scalars do not acquire mass of the order of the unification scale. One can be identified as the SM Higgs boson, whereas the other is an  $\text{SU}(2)_L$  singlet, which was not found so far. Finally, using the software MINUIT [21], we were able to find a set of parameters (shown in Table III) which not only respect the constraints imposed above but also fit pretty well the mass of the SM Higgs boson,  $m_H = 125.09 \pm 0.24$  GeV [8], with  $\chi^2 = 0.046$ .

<sup>2</sup> We use hats to designate complex VEVs.

Potential parameters	VEV parameters
$\alpha_1 = -0.18867$	$M_1 = 3.4640 \times 10^5 \text{ GeV}$
$\beta_1 = 0.47375$	$M_2 = 8.0296 \times 10^3 \text{ GeV}$
$\beta_2 = 0.55327$	$M_3 = 8.5884 \times 10^7 \text{ GeV}$
$\lambda_1 = 0.69314$	$\xi = \pi/2.0116$
$\lambda_3 = 0.01499$	
$\lambda_4 = -0.98621$	

TABLE III: Numerical values of the scalar potential and VEV parameters compatible with the observation of a SM Higgs boson with mass  $m_H \sim 125$  GeV. For this fit, we have obtained  $\chi^2 = 0.046$ .

### V. Fermion masses and mixing in the Trinification Model

We now turn our attention to the fermionic sector of our model. The Yukawa interactions with  $\phi_c$  and  $\chi_c$  are

$$\begin{aligned} \mathcal{L}_{\text{Yuk}} = & Y_\phi^q (\psi_{qL}^\dagger \phi_c^* \psi_{qR}^\dagger) + Y_\chi^q (\psi_{qL}^\dagger \chi_c^* \psi_{qR}^\dagger) \\ & + Y_\phi^\ell (\psi_\ell \psi_\ell \phi_c) + Y_\chi^\ell (\psi_\ell \psi_\ell \phi_c) + \text{cyclic} + \text{H.c.}, \end{aligned} \quad (47)$$

where  $Y_\phi^f$  and  $Y_\chi^f$  ( $f = q, \ell$ ) are real  $3 \times 3$  matrices (to ensure CP conservation), and the cyclic terms arise from the  $\mathbb{Z}_3$  symmetry we impose to the Lagrangian. As in Section II, the mass Lagrangian  $\mathcal{L}_{\text{Mass}}$  is obtained by evaluating Eq. (47) at the lowest-energy configuration of the scalar fields. We may write it as  $\mathcal{L}_{\text{Mass}} = \mathcal{L}_{\text{Mass}}^q + \mathcal{L}_{\text{Mass}}^\ell$ , with

$$\mathcal{L}_{\text{Mass}}^q = Y_\phi^q \psi_{qL}^\dagger \phi_c^* \psi_{qR}^\dagger + Y_\chi^q \psi_{qL}^\dagger \chi_c^* \psi_{qR}^\dagger + \text{H.c.}, \quad (48)$$

$$\mathcal{L}_{\text{Mass}}^\ell = Y_\phi^\ell \psi_\ell \psi_\ell \phi_c + Y_\chi^\ell \psi_\ell \psi_\ell \chi_c + \text{H.c.} \quad (49)$$

Focusing first on the quark mass Lagrangian, we may rewrite Eq. (48) as

$$\begin{aligned} \mathcal{L}_{\text{mass}}^q = & m_u (\bar{u}u) + m_d (\bar{d}d) + M' (\bar{d}B) \\ & + M (\bar{B}d) + M_B (\bar{B}B), \end{aligned} \quad (50)$$

in which  $m_u$  is the mass of the up- quarks,

$$m_u = Y_\phi^q \hat{v}_1 + Y_\chi^q \hat{b}_1. \quad (51)$$

For the down-type quarks, the mass matrix  $\mathcal{M}_d$  in the  $(d, B)$  basis is:

$$\mathcal{M}_d = \begin{pmatrix} m_d & M' \\ M & M_B \end{pmatrix}. \quad (52)$$

where the matrices  $m_d$ ,  $M'$ ,  $M$  and  $M_B$  are given by

$$\begin{aligned} m_d = & Y_\phi^q \hat{v}_2 + Y_\chi^q \hat{b}_2, & M_B = & Y_\phi^q \hat{M}_1 + Y_\chi^q \hat{M}_3, \\ M' = & Y_\chi^q \hat{b}_3, & M = & Y_\chi^q \hat{M}_2. \end{aligned} \quad (53)$$

From now on we consider the VEVs shown in Eqs. (43) and (44)<sup>3</sup>.

In order to study the quark mass and mixing pattern of our model, we start by computing the effective  $3 \times 3$  light down-quark matrix from Eq. (52). With this purpose, we introduce the Hermitian matrix

$$\mathcal{H}_d = \mathcal{M}_d \mathcal{M}_d^\dagger = \begin{pmatrix} m_d m_d^\dagger & m_d M^\dagger \\ M m_d^\dagger & M M^\dagger + M_B M_B^\dagger \end{pmatrix}, \quad (54)$$

and decouple the light down-quarks of the SM from the heavy vectorlike ones. This can be achieved by introducing a unitary matrix  $U$ ,

$$U^\dagger \mathcal{H}_d U = \begin{pmatrix} \mathcal{D}_d & 0 \\ 0 & \mathcal{D}_B \end{pmatrix}, \quad (55)$$

which leaves  $\mathcal{H}_d$  block-diagonal ( $\mathcal{D}_d$  and  $\mathcal{D}_B$  are  $3 \times 3$  matrices). For the matrix  $U$  we use the ansatz proposed in [22],

$$U = \begin{pmatrix} \sqrt{1 - FF^\dagger} & F \\ -F^\dagger & \sqrt{1 - F^\dagger F} \end{pmatrix}, \quad (56)$$

where  $F$  is also a matrix. Considering  $\sqrt{1 - FF^\dagger} \approx 1$  we can use Eq. (55) to compute  $F$ ,

$$F = m_d M^\dagger (M M^\dagger + M_B M_B^\dagger)^{-1}, \quad (57)$$

and insert it in Eq. (57) to compute  $\mathcal{D}_B$  and  $\mathcal{D}_d$ . Once we do this, we get for the former

$$\begin{aligned} \mathcal{D}_B = & Y_\phi^q Y_\phi^{q\dagger} M_1^2 + Y_\chi^q Y_\chi^{q\dagger} (M_2^2 + M_3^2) \\ & + \left[ Y_\phi^q Y_\chi^{q\dagger} M_1 M_3 e^{i\theta} + Y_\chi^q Y_\phi^{q\dagger} M_3 M_1 e^{-i\theta} \right], \end{aligned} \quad (58)$$

while in the limit  $\mathcal{D}_d \ll (M M^\dagger + M_B M_B^\dagger)$ , the effective down-quark mass matrix  $m_{\text{eff}}^q$  is defined by

$$m_{\text{eff}}^q m_{\text{eff}}^{q\dagger} \approx \mathcal{D}_d = v^2 \cos^2 \xi Y_\phi^q (\mathbb{1} - M_2^2 Y_\chi^{q\dagger} \mathcal{D}_B^{-1} Y_\chi^q) Y_\phi^{q\dagger}. \quad (59)$$

Here, we have already replaced  $m_d$ ,  $M$  and  $M_B$  by their form given in Eq. (53). From Eq. (59) we see that with no vectorlike quarks,  $m_{\text{eff}}^q$  would be similar to the SM one of Eq. (15). Therefore, Eqs. (58) and (59) reflect the influence of vectorlike quarks in the mass matrix of down-quarks, encoded in the second term of Eq. (59).

We can now diagonalize  $m_{\text{eff}}^q$  in order to obtain the CKM matrix, which is obviously affected by the presence of the  $B$  quarks. For this purpose, we work in a basis where the mass matrix of up-quarks is diagonal, implying [see Eq. (51)]

$$Y_\chi^q = \text{diag} \left( \frac{m_u}{v \sin \xi}, \frac{m_c}{v \sin \xi}, \frac{m_t}{v \sin \xi} \right). \quad (60)$$

<sup>3</sup> The VEV  $\hat{M}_3$  is often neglected [18–20]. Here we will not do this simplification, otherwise we could not have CP violation.

Quark masses
$m_u(M_Z) = 1.327 \pm 0.28$ MeV
$m_d(M_Z) = 2.769^{+0.33}_{-0.21}$ MeV
$m_s(M_Z) = 54.79 \pm 3.6$ MeV
$m_c(M_Z) = 0.6314 \pm 0.031$ GeV
$m_b(M_Z) = 2.861 \pm 0.045$ GeV
$m_t(M_Z) = 173 \pm 2.1$ GeV

TABLE IV: Masses of quarks computed at the electroweak scale  $M_Z = 91.1876 \pm 0.0021$  GeV (data taken from [23]).

We also take into account the definition for the CKM matrix given in Section II, being now the matrix which diagonalizes  $m_{\text{eff}}^q$ . Furthermore, the eigenvalues of the latter corresponds to the light down-quark masses. We performed a  $\chi^2$  minimization with respect to the four parameters of the CKM matrix (see Table I), as well as to the three down-quark masses, computed at the electroweak scale (Table IV). The fitted parameters are those of  $Y_\phi^q$ :

$$Y_\phi^q = \begin{pmatrix} y_{11} & y_{12} & y_{13} \\ y_{21} & y_{22} & y_{23} \\ y_{31} & y_{32} & y_{33} \end{pmatrix}, \quad (61)$$

being all real. As one can see from Table V, we only need seven of the nine free parameters to fit the seven observables (three CKM angles, one phase and three quark masses), with  $\chi^2 \ll 1$ .

The results shown in Tables III and V also allow us to make a prediction for the masses of the vectorlike quarks. Using the set of parameters where  $y_{11} = y_{13} = 0$  and taking into account that those masses correspond to the square root of the eigenvalues of  $\mathcal{D}_B$ , they are given by

$$m_{B1} \simeq 299 \text{ TeV}, \quad (62)$$

$$m_{B2} \simeq 313 \text{ TeV}, \quad (63)$$

$$m_{B3} \simeq 8.540 \times 10^4 \text{ TeV}. \quad (64)$$

All these values are above the current lower limit for the  $B$  quark mass (see Section III). Hence, we conclude that the predictions of our model are compatible with experimental constraints on vectorlike quark masses.

We now briefly study the lepton mass Lagrangian of the model. After replacing the fields  $\phi$  and  $\chi$  with the

Zero entries	Free parameters	$\chi^2$
	$y_{12}$	0.01291
	$y_{21}$	-0.00132
$y_{11}, y_{13}$	$y_{22}$	0.05688
	$y_{23}$	0.09017
	$y_{31}$	0.22826
	$y_{32}$	-0.09430
	$y_{33}$	-2.28568
	$y_{12}$	-0.01300
	$y_{13}$	-0.00143
$y_{11}, y_{32}$	$y_{22}$	0.00144
	$y_{23}$	0.05353
	$y_{31}$	0.09637
	$y_{32}$	-0.23123
	$y_{33}$	-2.29297
	$y_{12}$	0.01348
	$y_{13}$	-0.02034
$y_{11}, y_{21}$	$y_{21}$	0.07485
	$y_{22}$	0.03931
	$y_{23}$	0.19620
	$y_{31}$	0.48439
	$y_{33}$	3.11835

TABLE V: Fit of the effective down-quark matrix to the CKM parameters and down-quark masses given in Tables I and IV. The first column indicates the parameters of  $Y_\phi^q$  we set to zero.

VEVs in Eqs. (40) and (41), we may write<sup>4</sup>

$$\mathcal{L}_{\text{Mass}}^\ell = (\bar{e}_L \quad \bar{E}_L) \mathcal{M}_\ell^\pm \begin{pmatrix} e_R \\ E_R \end{pmatrix} + \left( \bar{E}_L^0 \quad \bar{N}_{2L} \quad \bar{\nu}_L \quad \bar{N}_{1L} \right) \mathcal{M}_\ell^0 \begin{pmatrix} E_R^0 \\ N_{2R} \\ \nu_R \\ N_{1R} \end{pmatrix}, \quad (65)$$

where  $\mathcal{M}_\ell^\pm$  and  $\mathcal{M}_\ell^0$  are the mass matrices of charged leptons and neutrinos, respectively:

$$\mathcal{M}_\ell^\pm = \begin{pmatrix} -Y_\phi^\ell \hat{v}_2 - Y_\chi^\ell \hat{b}_2 & Y_\chi^\ell \hat{b}_3 \\ Y_\chi^\ell \hat{M}_2 & -Y_\phi^\ell \hat{M}_1 - Y_\chi^\ell \hat{M}_3 \end{pmatrix}, \quad (66)$$

$$\mathcal{M}_\ell^0 = \begin{pmatrix} Y_\phi^\ell \hat{M}_1 + Y_\chi^\ell \hat{M}_3 & Y_\phi^\ell \hat{v}_1 + Y_\chi^\ell \hat{b}_1 & 0 & 0 \\ Y_\phi^\ell \hat{v}_2 + Y_\chi^\ell \hat{b}_2 & 0 & 0 & 0 \\ -Y_\chi^\ell \hat{b}_3 & 0 & 0 & -Y_\phi^\ell \hat{v}_1 - Y_\chi^\ell \hat{b}_1 \\ -Y_\chi^\ell \hat{M}_2 & 0 & -Y_\phi^\ell \hat{v}_1 - Y_\chi^\ell \hat{b}_1 & 0 \end{pmatrix}. \quad (67)$$

<sup>4</sup> In order to write the lepton mass matrices, one should take into account in Eq. (49) that  $\psi_\ell = C \bar{\psi}_\ell^T$ , where  $C$  is the charge conjugation operator.

Apart from the different Yukawa matrices and overall signs, the matrix  $\mathcal{M}_\ell^\pm$  is similar to the down-quark one,  $\mathcal{M}_d$ . Then, using the VEVs shown in Eqs. (43) and (44), the results we obtain after diagonalizing  $\mathcal{M}_\ell^\pm$  are similar to those presented in Eqs. (58) and (59), as long as we perform the replacements  $Y_\phi^q \rightarrow Y_\phi^\ell$  and  $Y_\chi^q \rightarrow Y_\chi^\ell$ . Considering the case where both Yukawa matrices of the leptonic sector are diagonal,

$$\begin{aligned} Y_\phi^\ell &= \text{diag}(y_{\phi_1}, y_{\phi_2}, y_{\phi_3}), \\ Y_\chi^\ell &= \text{diag}(y_{\chi_1}, y_{\chi_2}, y_{\chi_3}), \end{aligned} \quad (68)$$

one can notice that charged leptons do not need to couple to the field  $\chi$  to become massive.

## VI. Conclusions

In spite of some limitations, the SM is a theory in remarkable agreement with most experimental results. For this reason, one of the challenges we face putting forward a new theory is to guarantee that, at low energies, it delivers similar predictions to the ones given by the SM. This was our main motivation to study Trinification models.

After reviewing the SM in Section II, we were able to understand in Section III why models with vectorlike quarks are so attractive. One of the features we most emphasized is the possibility of having mixing with SM quarks. Even if we are not able to observe vectorlike quarks directly in the near future (we know already that

if they exist their mass is at least of the order of TeV-scale), the effects of this mixing may provide an indirect evidence for their existence. Also, heavy-light quark mixing must be compatible with the oblique parameters  $S$  and  $T$ , and with the observables related to the  $Zb\bar{b}$  coupling.

The most interesting results of our work have been presented in Sections IV and V. Namely, we were able to fit the many free parameters of the Trinification model to obtain the SM Higgs boson mass, as well as the CKM matrix and quark masses. We achieved a valid scalar mass spectrum which, along with the mass of the Higgs boson, it predicts the correct number of massive neutral and charged scalar particles. Concerning CKM mixing, we noticed that the effective down-quark mass matrix contains one term related to the mixing between vectorlike and SM quarks. We concluded that this feature leads to a CKM pattern compatible with all measurements related to CP violation at low energies.

Our findings have shown that Trinification models are valid SM extensions, at least from the point of view of quark masses, mixing and CP violation. Although we have not analyzed in detail the lepton sector, it would be interesting to investigate whether the present results on neutrino masses and mixing coming from neutrino oscillation experiments [24] could be reproduced in our model. This is a relevant and crucial question since neutrino masses can be accommodated in the present scenario via a seesaw mechanism [25–29]. Given this, we will further explore this possibility in the future.

- 
- [1] A. D. Sakharov, *Pisma Zh. Eksp. Teor. Fiz.* **5**, 32 (1967).  
[2] S. L. Glashow, in *Fifth Workshop on Grand Unification Providence, Rhode Island, April 12-14, 1984* (1984), p. 88.  
[3] J. A. Aguilar-Saavedra, R. Benbrik, S. Heinemeyer, and M. Pérez-Victoria, *Phys. Rev. D* **88**, 094010 (2013), 1306.0572.  
[4] N. Cabibbo, *Phys. Rev. Lett.* **10**, 531 (1963).  
[5] M. Kobayashi and T. Maskawa, *Prog. Theor. Phys.* **49**, 652 (1973).  
[6] L. Wolfenstein, *Phys. Rev. Lett.* **51**, 1945 (1983).  
[7] A. J. Buras, M. E. Lautenbacher, and G. Ostermaier, *Phys. Rev. D* **50**, 3433 (1994), hep-ph/9403384.  
[8] C. Patrignani *et al.* (Particle Data Group), *Chin. Phys. C* **40**, 100001 (2016).  
[9] A. Djouadi and A. Lenz, *Phys. Lett. B* **715**, 310 (2012), 1204.1252.  
[10] J. Beringer *et al.* (Particle Data Group), *Phys. Rev. D* **86**, 010001 (2012).  
[11] S. Schael *et al.* (SLD Electroweak Group, DELPHI, ALEPH, SLD, SLD Heavy Flavour Group, OPAL, LEP Electroweak Working Group, L3), *Phys. Rep.* **427**, 257 (2006), hep-ex/0509008.  
[12] S. Dawson and E. Furlan, *Phys. Rev. D* **86**, 015021 (2012), 1205.4733.  
[13] M. Aaboud *et al.* (ATLAS Collaboration) (ATLAS Collaboration), Report No. CERN-EP-2017-094 (2017), 1707.03347.  
[14] G. Aad *et al.* (ATLAS Collaboration), Report No. ATLAS-CONF-2013-051 (2013), URL <http://cds.cern.ch/record/1547567>.  
[15] S. Willenbrock, *Phys. Lett. B* **561**, 130 (2003), hep-ph/0302168.  
[16] J. Hetzel, Ph.D. thesis, Inst. Appl. Math., Heidelberg (2015), 1504.06739, URL <http://inspirehep.net/record/1364898/files/arXiv:1504.06739.pdf>.  
[17] H. Georgi, *Lie Algebras In Particle Physics: from Isospin To Unified Theories*, Frontiers in Physics (Avalon Publishing, 1999), ISBN 9780813346113, URL <https://books.google.pt/books?id=g4yEuH5rBMUC>.  
[18] K. S. Babu, X.-G. He, and S. Pakvasa, *Phys. Rev. D* **33**, 763 (1986).  
[19] J. Sayre, S. Wiesenfeldt, and S. Willenbrock, *Phys. Rev. D* **73**, 035013 (2006), hep-ph/0601040.  
[20] C. Cautet, H. Pas, and S. Wiesenfeldt, *Phys. Rev. D* **83**, 093008 (2011), 1012.4083.  
[21] F. James and M. Roos, *Comput. Phys. Commun.* **10**, 343 (1975), URL <https://cds.cern.ch/record/310399>.  
[22] W. Grimus and L. Lavoura, *JHEP* **11**, 042 (2000), hep-ph/0008179.

- [23] D. Emmanuel-Costa and R. González Felipe, *Phys. Lett. B* **764**, 150 (2017), 1609.09491.
- [24] G. C. Branco, R. G. Felipe, and F. R. Joaquim, *Rev. Mod. Phys.* **84**, 515 (2012), 1111.5332.
- [25] P. Minkowski, *Phys. Lett. B* **67**, 421 (1977).
- [26] T. Yanagida, In *Proceedings of the Workshop on the Baryon Number of the Universe and Unified Theories*, 13-14 February 1979, Tsukuba, Japan (1979).
- [27] M. Gell-Mann, P. Ramond, and R. Slansky, In *Supergravity*, P. van Nieuwenhuizen and D.Z. Freedman (eds.), North Holland Publ. Co. p. 315 (1979).
- [28] S. L. Glashow, *Quarks and Leptons*, in *Cargèse Lectures*, eds. M. Lévy et al., Plenum, NY p. 687 (1980).
- [29] R. N. Mohapatra and G. Senjanovic, *Phys. Rev. Lett.* **44**, 912 (1980).